Supporting Information for:
Dinuclear Ligand-to-Ligand Charge Transfer Complexes

David A. Shultz,*[1] Riley Stephenson,[1] and Martin L. Kirk2,3,4
[1]Department of Chemistry, North Carolina State University, Raleigh, North Carolina, 27695-8204; [2]Department of Chemistry and Chemical Biology, The University of New Mexico, MSC03 2060, 1 University of New Mexico, Albuquerque, NM 87131-0001. [3]The Center for High Technology Materials, The University of New Mexico, Albuquerque, New Mexico 87106, United States. [4]Center for Quantum Information and Control (CQuIC), The University of New Mexico, Albuquerque, New Mexico 87131-0001

Table of Contents

Considerations for Spectroscopy and Electrochemistry

Nuclear Magnetic Resonance Spectroscopy

^{1}H NMR (400 or 600 MHz) spectra, ^{13}C NMR (101 MHz), and NOESY (400 MHz) spectra were acquired at room temperature in $CDCl_3$ or DMSO-d_6. Chemical shifts (δ) are reported in parts per million (ppm) using residual protonated solvent as the internal reference.

Electronic Absorption Spectroscopy

Electronic absorbance spectra were taken on a Shimadzu UV-1800 Spectrophotometer. To obtain molar extinction coefficients, five dilute samples in CH_2Cl_2 were prepared with LL'CT bands between 0.1 – 1.0 absorbance units. Then, the electronic absorbance spectra were obtained, and the molar extension coefficients were calculated via the Beer-Lambert law**.**

High Resolution Mass Spectrometry

High resolution mass spectra were acquired using a *Thermo Fisher Scientific Exactive Plus MS* - a benchtop full-scan Orbitrap™ mass spectrometer – using Heated Electrospray Ionization (HESI). Samples were dissolved in methylene chloride and acetonitrile and analyzed via flow injection into the mass spectrometer at a flow rate of 200 μL/min. The mobile phase was 90% acetonitrile with 0.1% formic acid and 10% water with 0.1% formic acid. The mass spectrometer was operated in positive and negative ion modes. Samples were analyzed via flow injection into the mass spectrometer at a flow rate of 8 μL/min**.**

Ultrafast Transient Absorption Spectroscopy

Ultrafast transient absorption spectra were obtained using a standard pump-probe technique. Optical pulses (~80 fs) centered at 800 nm were generated using a Ti:sapphire laser (Solstice Ace, Spectra-Physics), which consists of a regenerative amplifier seeded by a mode-locked fiber oscillator. An optical parametric amplifier (TOPAS-C; Light Conversion) was used to tune the excitation pulse to 640 nm to excite the (bpy)Pt(CAT) ligand-to-ligand charge transfer transitions. The excitation energy was measured to be 0.549 μJ/pulse. Using a custom built HARPIA-TA (Light Conversion) system, the pump beam was chopped a quarter of the laser repetition rate (~250 Hz) to alternatively block and transmit a pair of pulses. A fraction of the output from the regenerative amplifier was passed through an optical delay line and focused onto a sapphire crystal which was continuously translated in a circular pattern to generate a white-light continuum used as the probe beam. Pump/probe polarization was set to magic angle (54.7°) for these experiments. After passing through the sample, the probe light was focused onto a Kymera 328i spectrograph (Andor, Oxford Instruments). The samples were prepared in degassed CH_2Cl_2 in a 2 mm air-free quartz cuvette via a freeze-pump-thaw technique (x3). The cuvette was then refilled with argon. All transient spectra reported represent averages obtained over three scans for a total of 7500 difference spectra per time delay. These data were analyzed utilizing CarpetView software (Light Conversion). Using this software, the spectral range between 600-700 nm (predominantly excitation laser scattering) was removed and the data were corrected for dispersion (chirp) before further analysis. The data were then adjacently averaged and binned to the 2 nearest neighbor spectral and time points before kinetic fitting. 3D surface plots and select kinetic traces of the transient absorption data are displayed in ***Figure S1***.

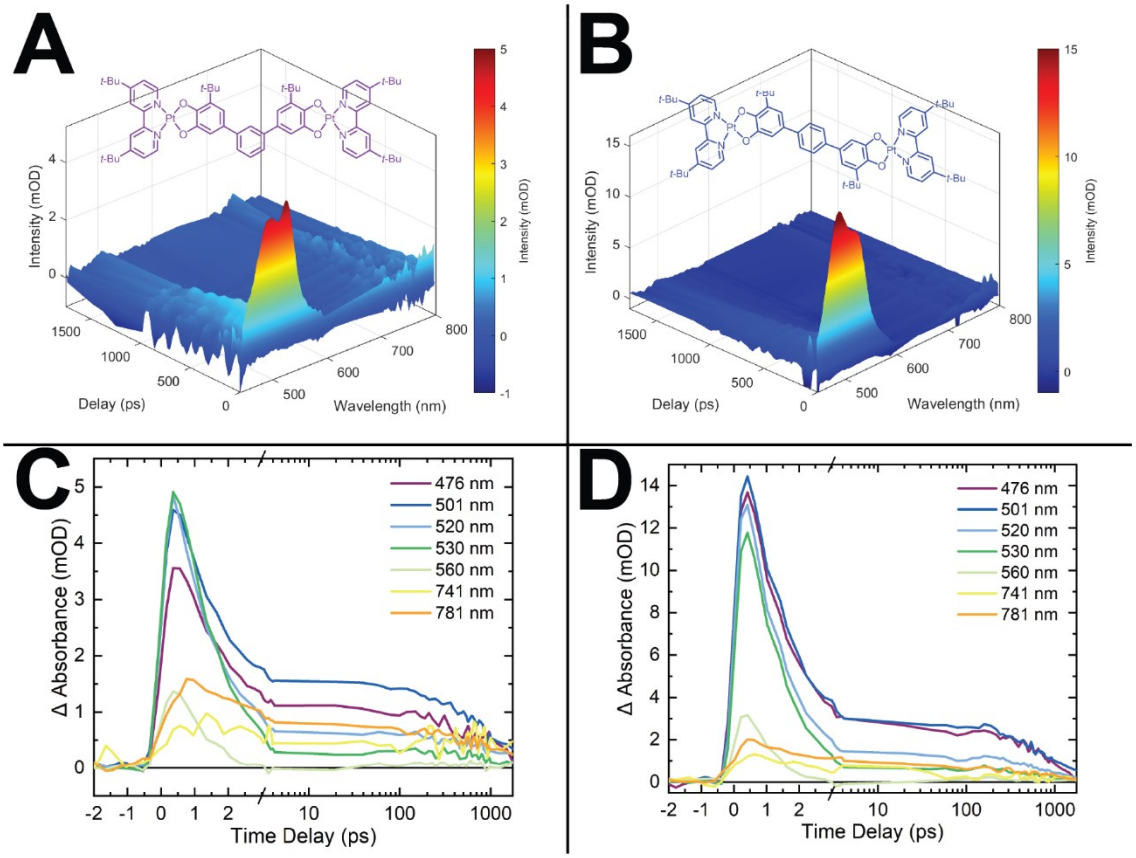

Figure S1. 3D surface plots of transient absorption data (plotted in linear space from -10 to 1750 ps time delays) of **A.)** ***m*-Ph[(CAT)Pt(bpy)]$_2$** and **B.)** ***p*-Ph[(CAT)Pt(bpy)]$_2$** and select kinetic traces of **C.)** ***m*-Ph[(CAT)Pt(bpy)]$_2$** and **D.)** ***p*-Ph[(CAT)Pt(bpy)]$_2$.**

To obtain kinetic lifetimes, the transient spectral data between 560-640nm (most prominent transient absorption spectral range for the (bpy)Pt(CAT) chromophores) were fit globally to two exponential lifetimes using a sequential model. The resulting evolution associated difference spectra (EADS) and global fit residuals are shown in ***Figure S2***.

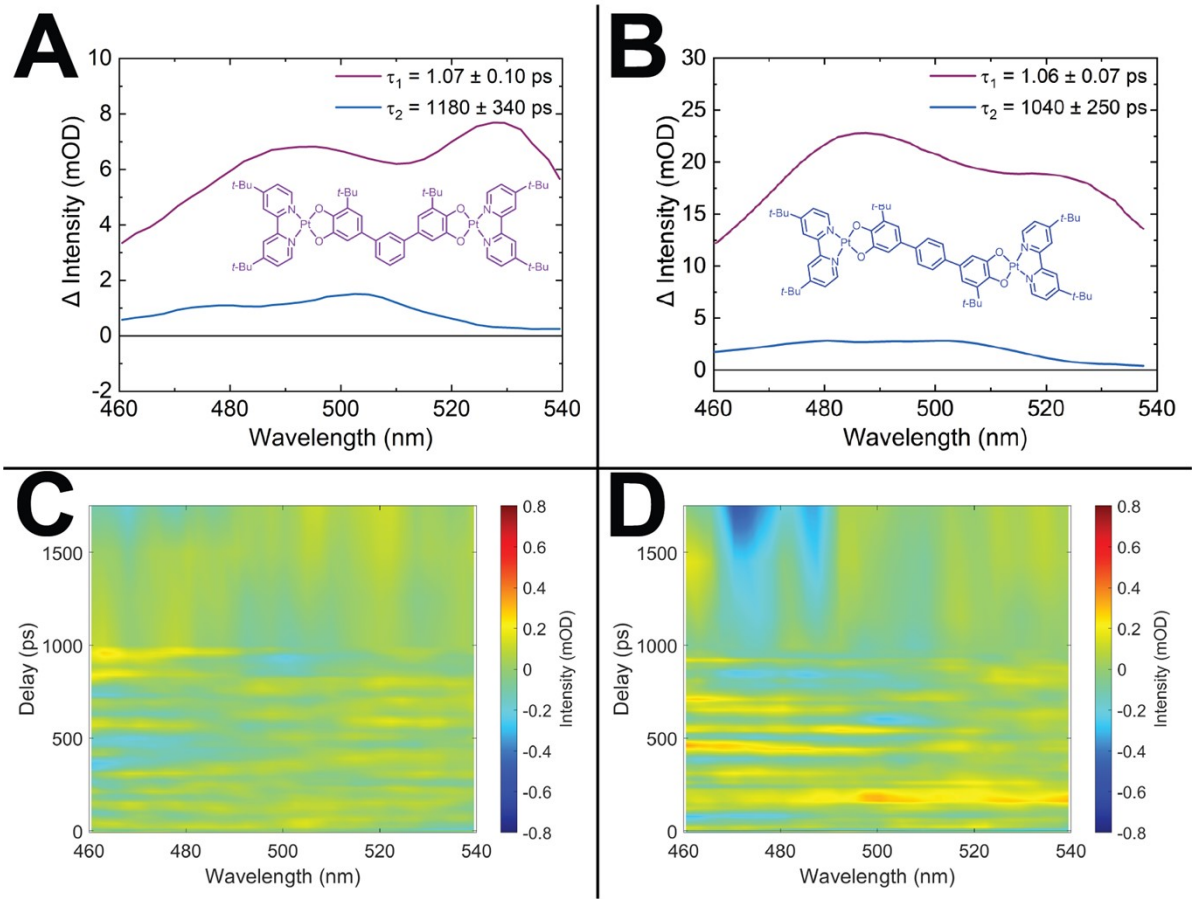

Figure S2. Evolution associated difference spectra and time constants generated from a sequential model global fitting to transient absorption data of **A.)** ***m*-Ph[(CAT)Pt(bpy)]$_2$** and **B.)** ***p*-Ph[(CAT)Pt(bpy)]$_2$** and 3D residual plot of global fit to the transient absorption data of **C.)** ***m*-Ph[(CAT)Pt(bpy)]$_2$** and **D.)** ***p*-Ph[(CAT)Pt(bpy)]$_2$.**

Electrochemistry

Cyclic voltammograms and differential pulse voltammograms were taken on a Bio-logic SAS SP 200 potentiostat monitored through EC-Lab. A three-electrode system of a glassy carbon working electrode, a platinum auxiliary electrode, and a silver wire reference electrode were used. Samples were prepared by placing ~4 mg of sample and ~387 mg of tetrabutylammonium hexafluorophosphate in a small glass vial fitted with a rubber septum. This vial was then purge/pumped on a Schlenk line with N_2 for three minutes under vacuum (x3). Then 10mL of distilled and degassed CH_2Cl_2 was added via an air-free syringe transfer. The electrodes were then added to the solution by removing the rubber septum while blowing argon over the cell. Cyclic voltammograms were obtained at a scan rate of 100 mV/s. Differential pulse voltammograms were obtained with a pulse height of 2.5 mV, a pulse width of 100 ms, a step height of 5 mV, and a step time of 500 ms. Argon was blown over the cell during each measurement to ensure inert conditions (Note: Ar was blow lightly to prevent production of current due to convection). All voltammograms are referenced to the ferrocene/ferrocenium redox couple by spiking each solution with ferrocene after the initial measurements and obtaining a second set of voltammograms of the sample. Ferrocene and tetrabutylammonium hexafluorophosphate were purified before use via sublimation and recrystallization out of ethanol (x3) respectively.

Synthesis and Characterization

All products were synthesized with reagents and solvents that were obtained from commercial sources and used without further purification.

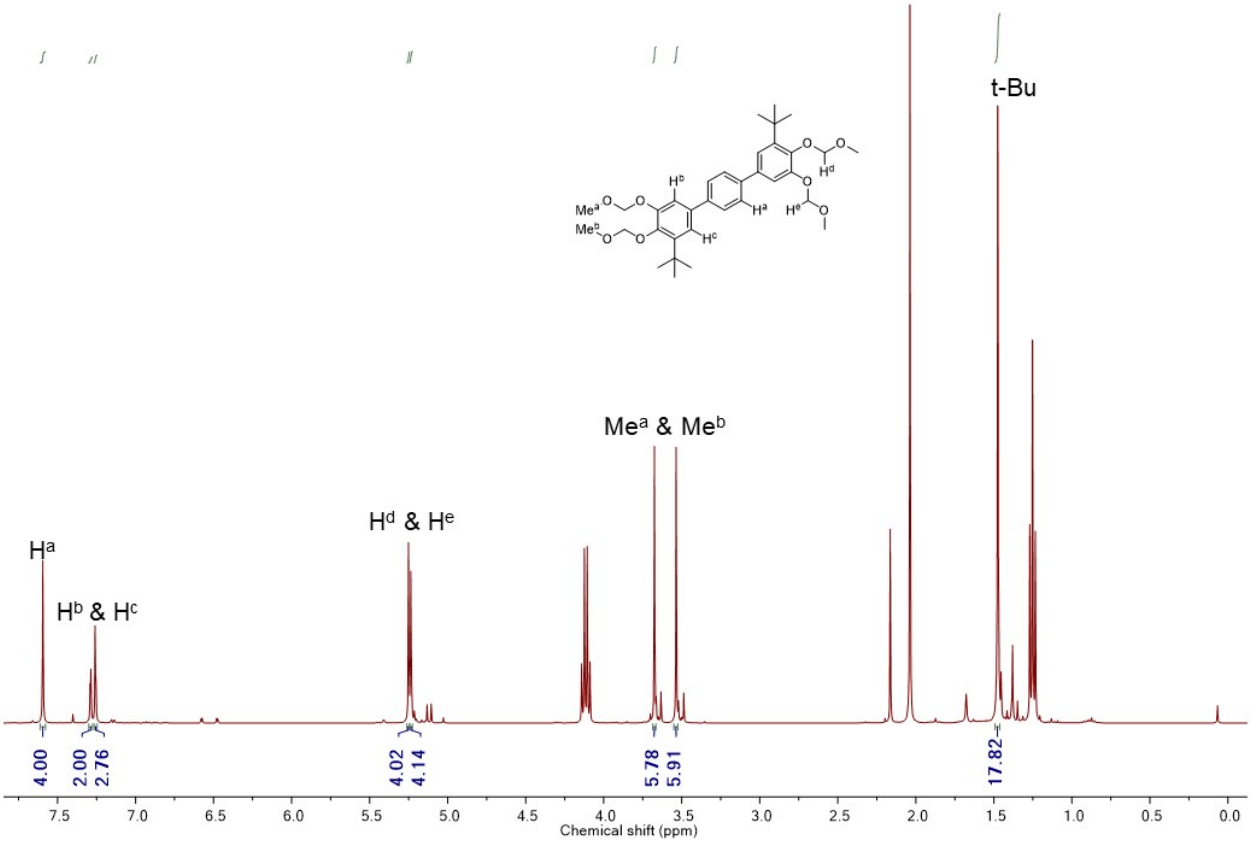

Figure S3. ^{1}H NMR spectrum of 3,3"-di-*tert*-butyl-4,4",5,5"-tetrakis(methoxymethoxy)-1,1':4',1"-terphenyl (***p*-Ph(CAT(MOM)$_2$)$_2$**). ^{1}H NMR (400 MHz, Chloroform-*d*) δ 7.59 (s, 4H), 7.29 (d, *J* = 2.1 Hz, 2H), 7.26 (d, *J* = 2.1 Hz, 2H), 5.25 (s, 4H), 5.24 (s, 4H), 3.68 (s, 6H), 3.54 (s, 6H), 1.47 (s, 18H). Impurities: acetone (2.16 ppm), 1,4-diiodobenzene (7.40 ppm), ethyl acetate (4.12, 2.04, 1.25 ppm), hexanes (0.87), silicone grease (0.07 ppm), unknown impurities (7.15, 7.14, 5.41, 5.13, 5.11, 5.03, 3.70, 3.66, 3.63, 3.52, 3.49, 1.68, 1.45, 1.38).

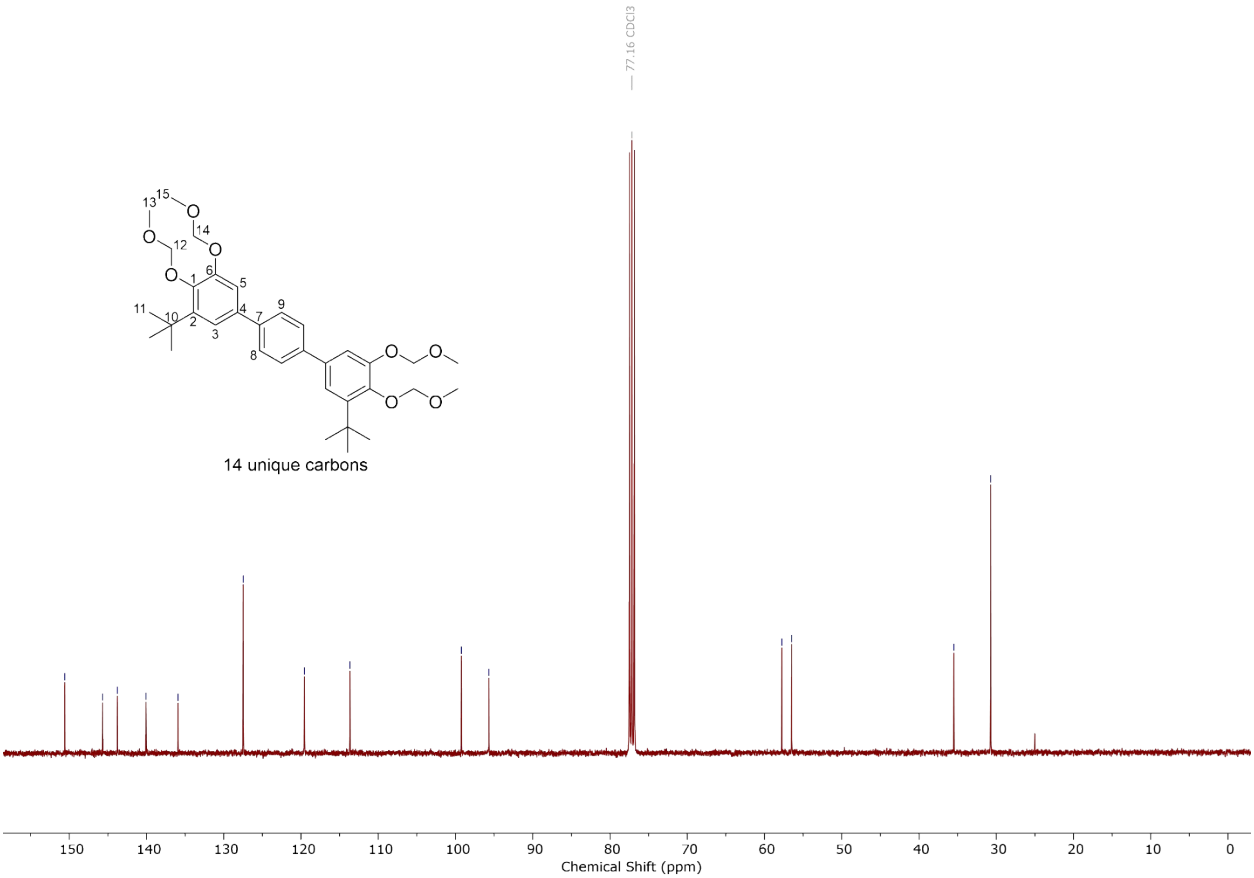

Figure S4. ^{13}C NMR spectrum of 3,3"-di-*tert*-butyl-4,4",5,5"-tetrakis(methoxymethoxy)-1,1':4',1"-terphenyl (***p*-Ph(CAT(MOM)$_2$)$_2$**).^{13}C NMR (101 MHz, $CDCl_3$) δ 150.58, 145.68, 143.78, 140.07, 135.92, 127.48, 119.56, 113.66, 99.24, 95.68, 57.75, 56.48, 35.48, 30.71.

A.)

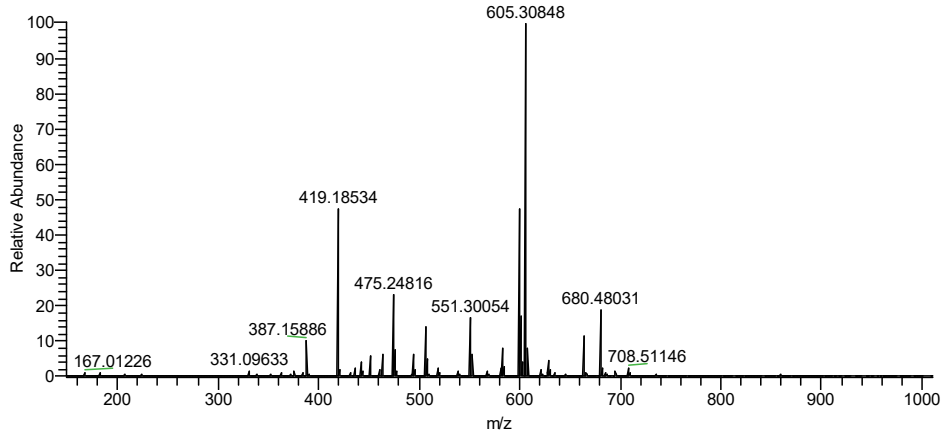

B.)

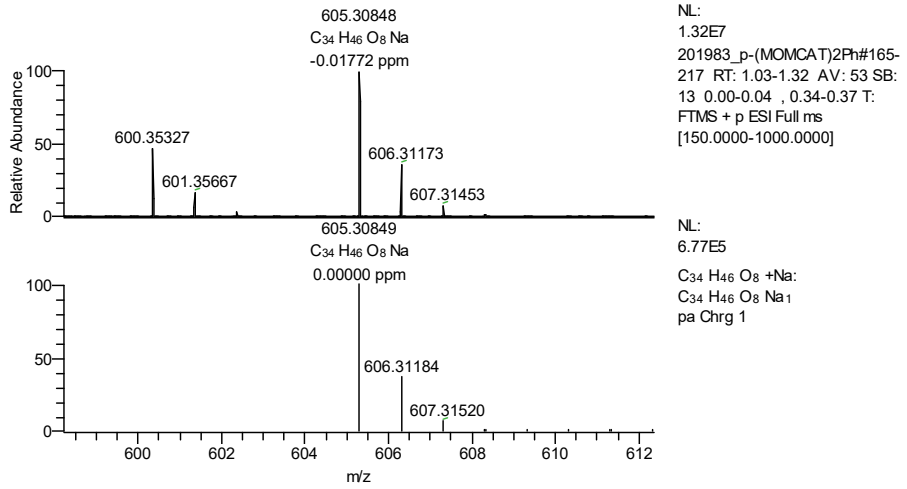

Figure S5. HRMS (ESI) data for 3,3"-di-*tert*-butyl-4,4",5,5"-tetrakis(methoxymethoxy)-1,1':4',1"-terphenyl (***p*-Ph(CAT(MOM)$_2$)$_2$**). HRMS (ESI) m/z: $[M+Na]^+$ Calcd for $C_{34}H_{46}O_8$ 605.30849; Found 605.30848. **A.)** Full scan Positive ion mode. **B.)** Experimental and theoretical isotopic distribution for $C_{34}H_{46}O_8$ $[M+Na]^+$.

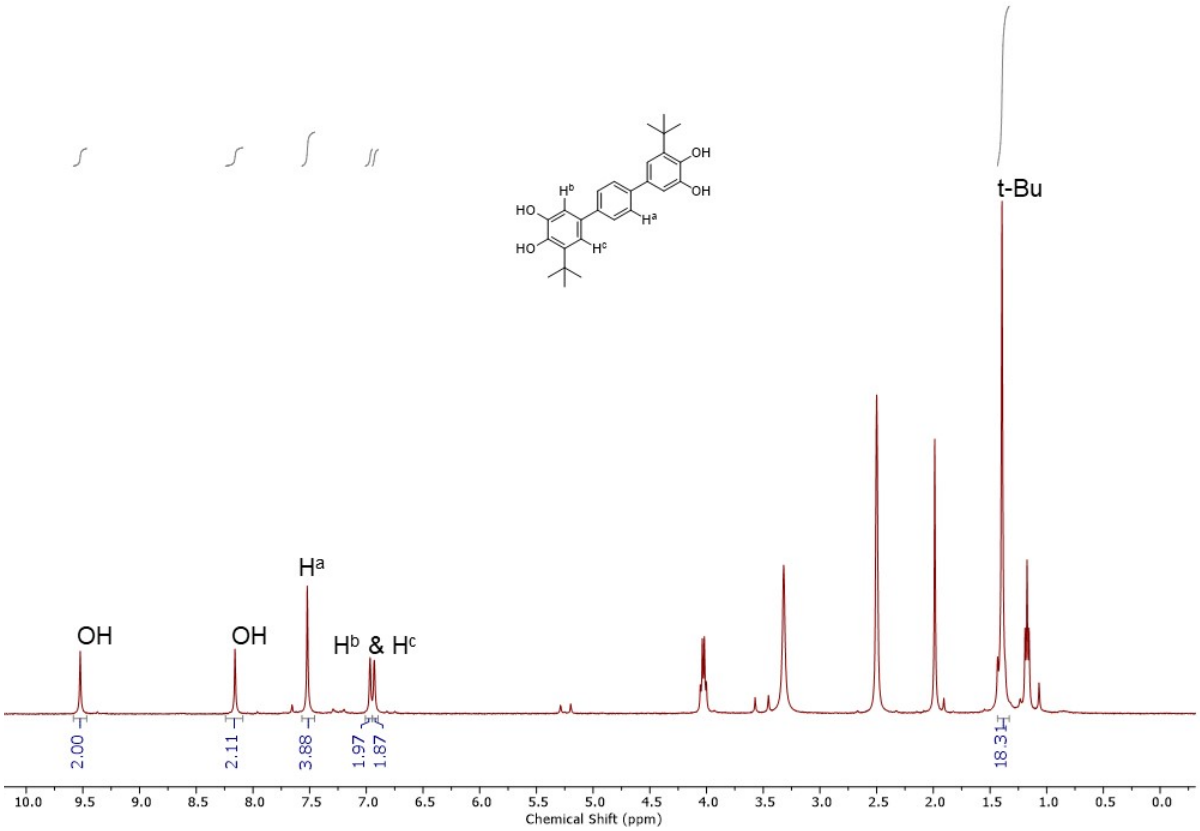

Figure S6. ^{1}H NMR spectrum of 5,5"-di-*tert*-butyl-[1,1':4',1"-terphenyl]-3,3",4,4"-tetraol (***p*-Ph(CATH$_2$)$_2$**). ^{1}H NMR (400 MHz, DMSO) δ 9.52 (s, 2H), 8.16 (s, 2H), 7.52 (s, 4H), 6.97 (s, 2H), 6.93 (s, 2H), 1.39 (s, 18H). Impurities: ethyl acetate (4.03, 1.99, 1.17 ppm), water (3.32 ppm), unknown impurities (9.37, 7.96, 7.66, 7.29, 7.20, 6.82, 6.75, 5.29, 5.20, 3.57, 3.45, 1.91, 1.43, 1.23, 1.07 ppm).

A.)

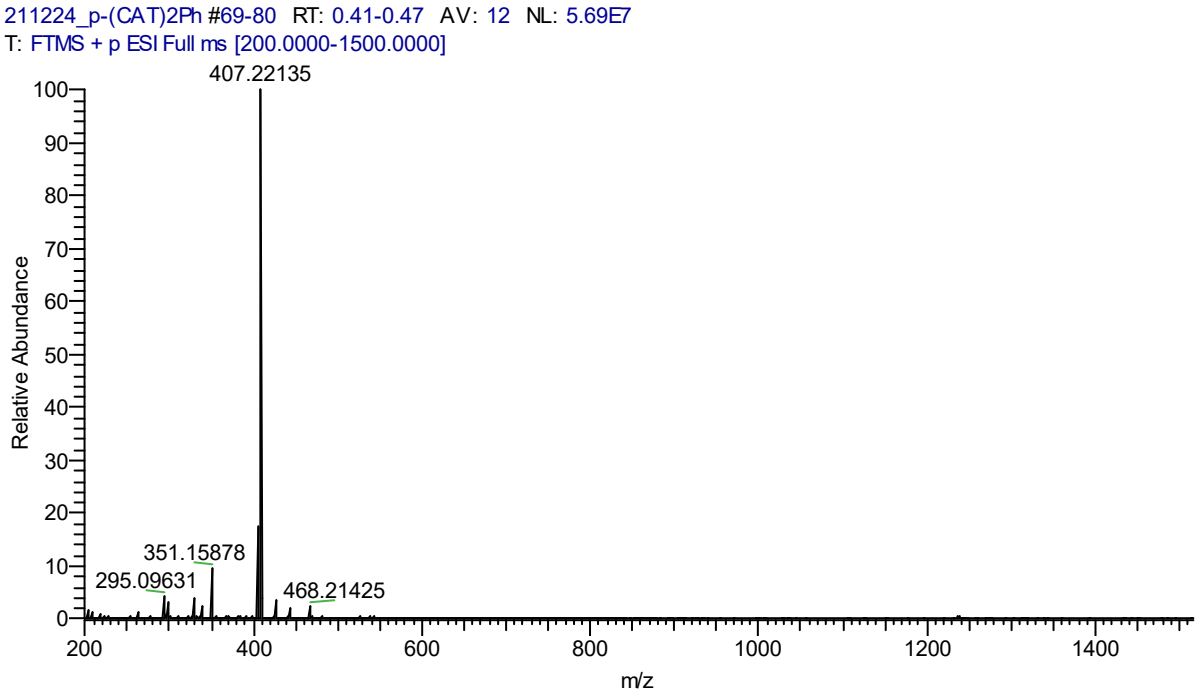

B.)

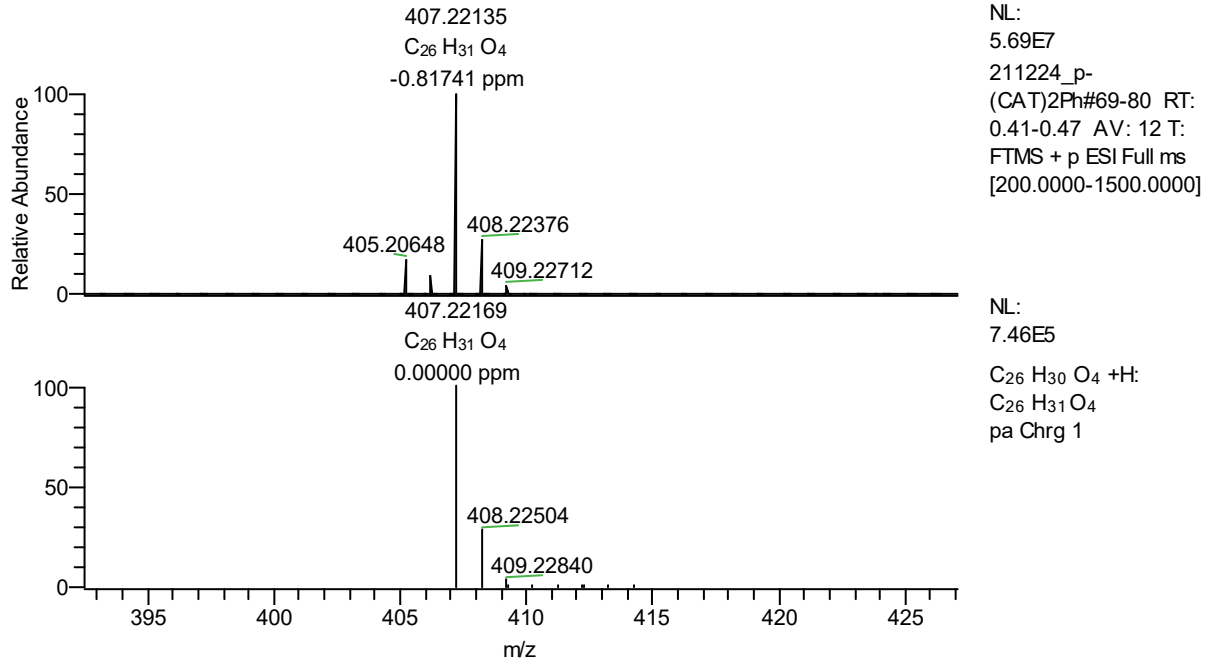

Figure S7. HRMS (ESI) data for 5,5"-di-*tert*-butyl-[1,1':4',1"-terphenyl]-3,3",4,4"-tetraol (***p*-Ph(CATH$_2$)$_2$**). HRMS (ESI) m/z: $[M+H]^+$ Calcd for $C_{26}H_{30}O_4$ 407.22169; Found 407.22135. **A.)** Full scan Positive ion mode. **B.)** Experimental and theoretical isotopic distribution for $C_{26}H_{30}O_4$ $[M+H]^+$.

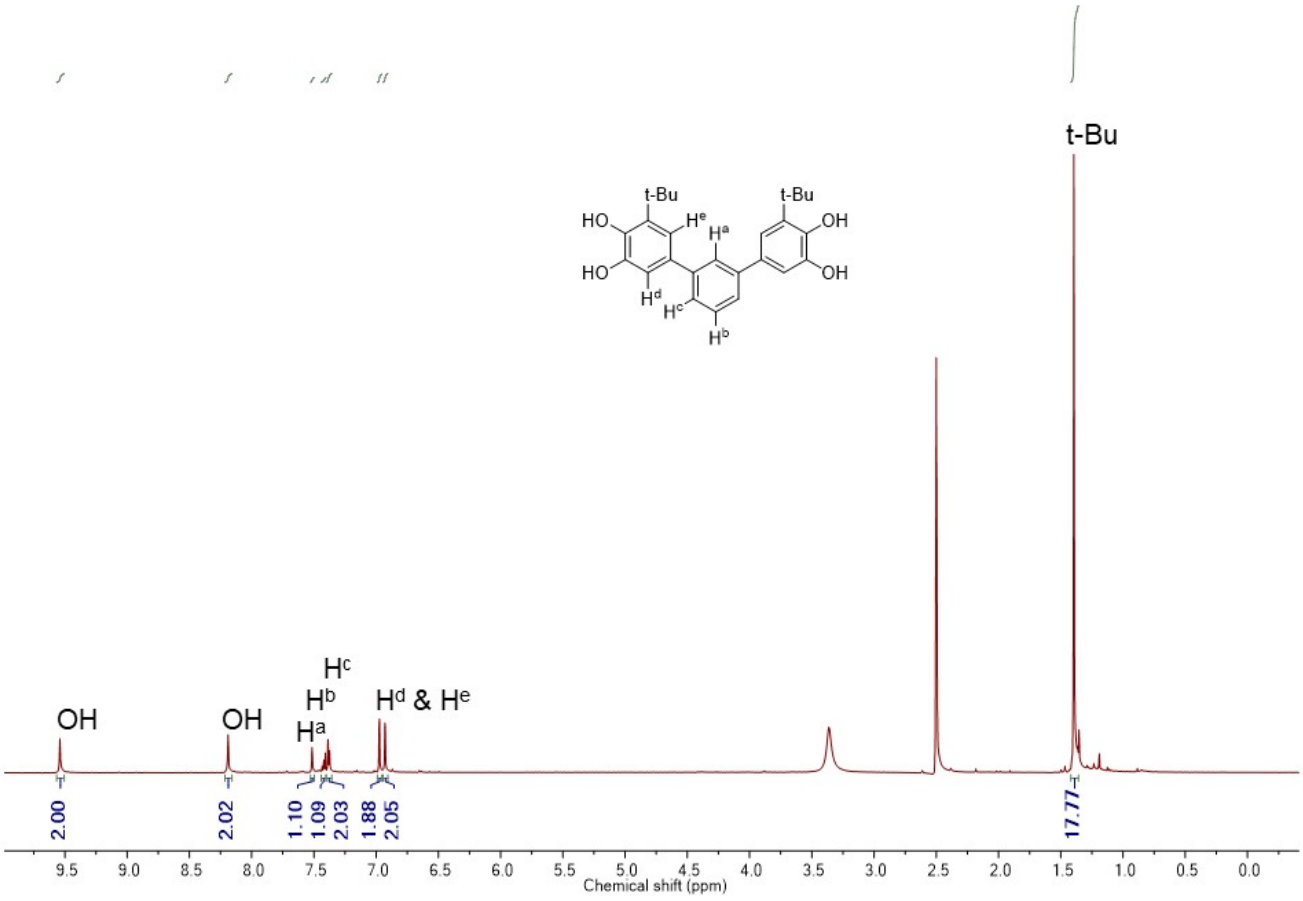

Figure S8. ^{1}H NMR spectrum of 5,5"-di-tert-butyl-[1,1':3',1"-terphenyl]-3,3",4,4"-tetraol (***m*-Ph(CATH$_2$)$_2$**) ^{1}H NMR (600 MHz, DMSO-d_6) δ 9.54 (s, 2H), 8.19 (s, 2H), 7.51 (s, 1H), 7.42 (dd, J = 8.7, 6.3 Hz, 1H), 7.40 – 7.36 (m, 2H), 6.97 (d, J = 2.1 Hz, 2H), 6.93 (d, J = 2.1 Hz, 2H), 1.40 (s, 18H). Impurities: water (3.36 ppm), unknown impurites (1.35, 1.19 ppm).

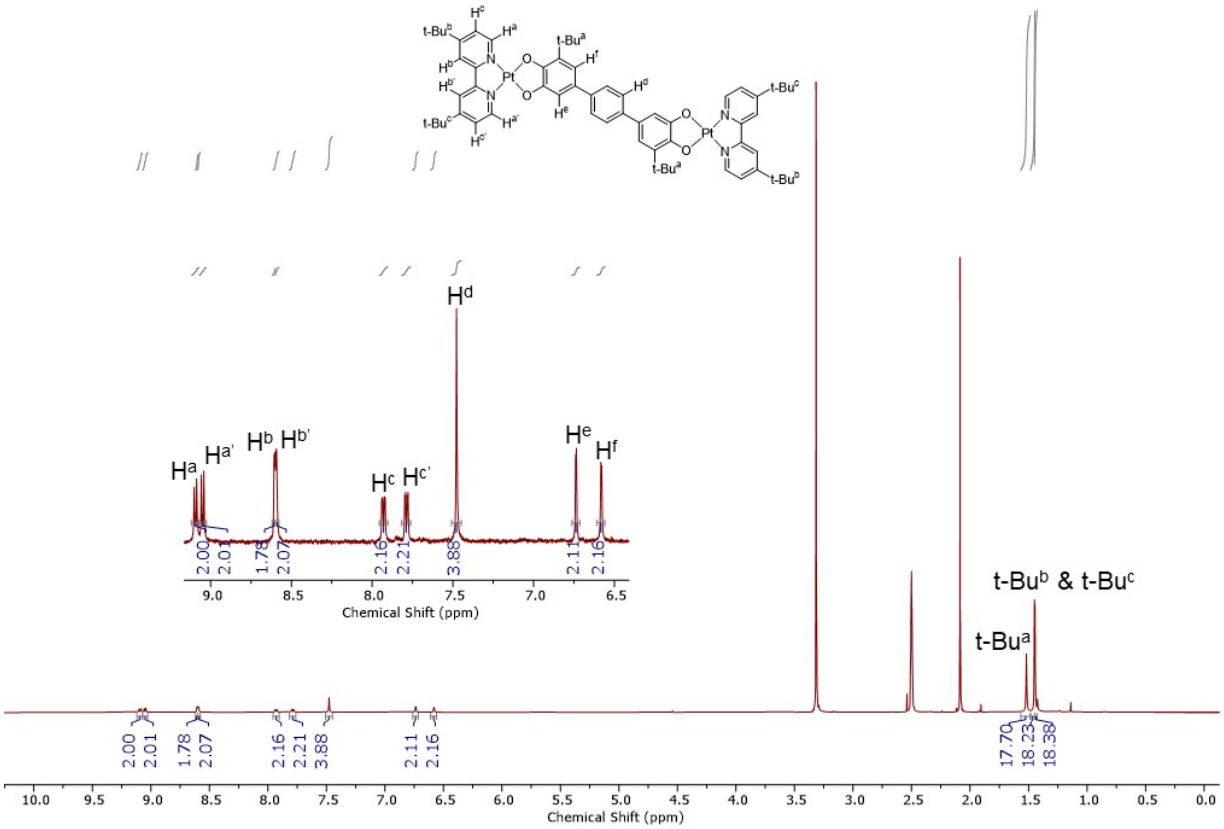

Figure S9. ^{1}H NMR spectrum of ***p*-Ph[(CAT)Pt(bpy)]$_2$**. ^{1}H NMR (400 MHz, DMSO) δ 9.09 (d, J = 6.00 Hz, 2H), 9.05 (d, J = 6.25 Hz, 2H), 8.60 (d, J = 1.88 Hz, 2H), 8.59 (d, J = 1.63 Hz, 2H), 7.93 (dd, J = 6.28, 1.90 Hz, 2H), 7.79 (dd, J = 6.25, 2.00 Hz, 2H), 7.48 (s, 4H), 6.74 (d, J = 2.13 Hz, 2H), 6.58 (d, J = 2.38 Hz, 2H), 1.52 (s, 18H), 1.45 (s, 18H), 1.45 (s, 18H). Impurities: acetone (2.08 ppm), dichloromethane (5.75 ppm), dimethyl sulfoxide (2.54 ppm), water (3.31 ppm), unknown impurites (9.37, 9.36, 4.54, 1.42, 1.14 ppm).

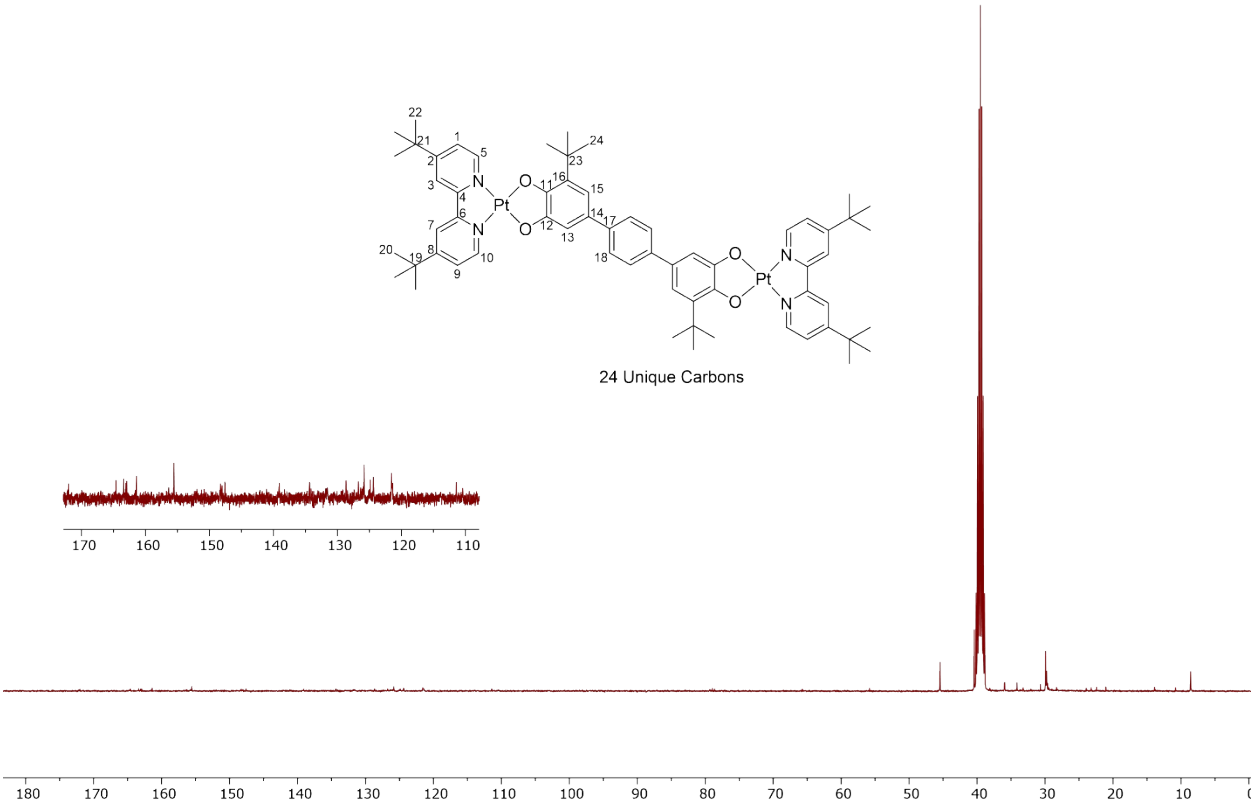

Figure S10. ^{13}C NMR spectrum of ***p*-Ph[(CAT)Pt(bpy)]$_2$**. ^{13}C NMR (101 MHz, DMSO) δ 171.99, 164.61, 163.38, 163.07, 162.92, 161.40, 155.55, 148.28, 147.57, 139.08, 134.36, 128.66, 126.73, 125.83, 124.90, 124.38, 121.55, 111.41, 35.98, 35.92, 34.14, 30.69, 29.91, 29.78, 29.76.

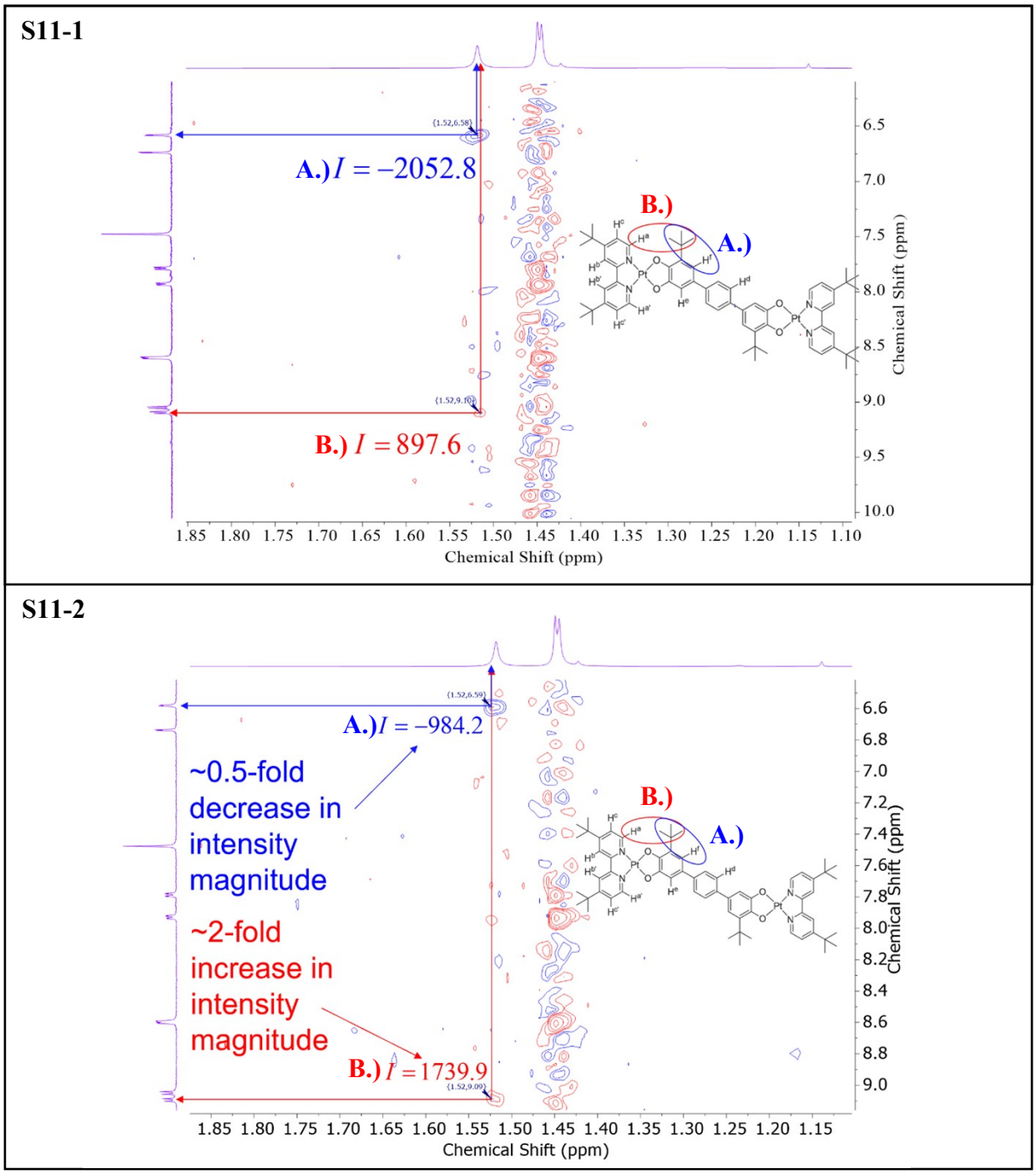

Figure S11. 2D NOESY spectra of ***p*-Ph[(CAT)Pt(bpy)]$_2$** in DMSO-d_6 displaying **A.)** a NOE cross peak (1.52, 6.59 ppm) showing the dipole-dipole relaxation interaction between protons ortho to the catecholate tert-Butyl group and the catecholate tert-Butyl protons and **B.)** a NOE cross peak (1.52, 9.09 ppm) showing the dipole-dipole relaxation interaction between protons in the bipyridine 6 position and the catecholate tert-Butyl protons. **S11-1** is a spectrum taken with twice the mixing time of **S11-2**.

A.)

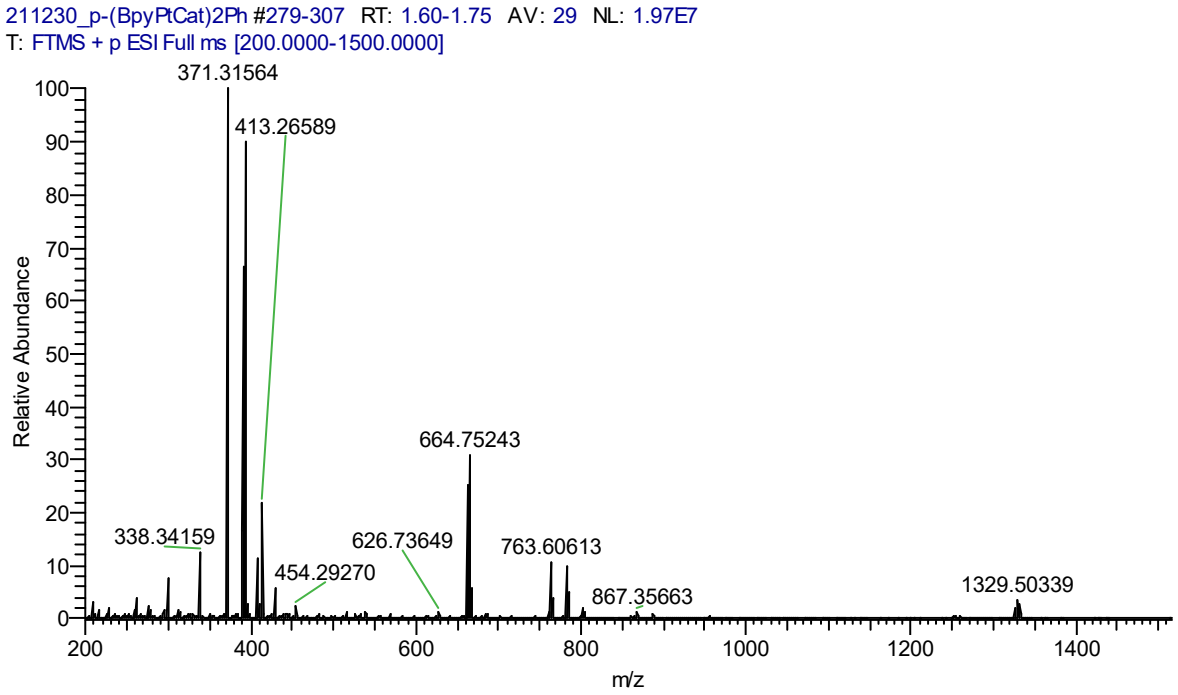

B.)

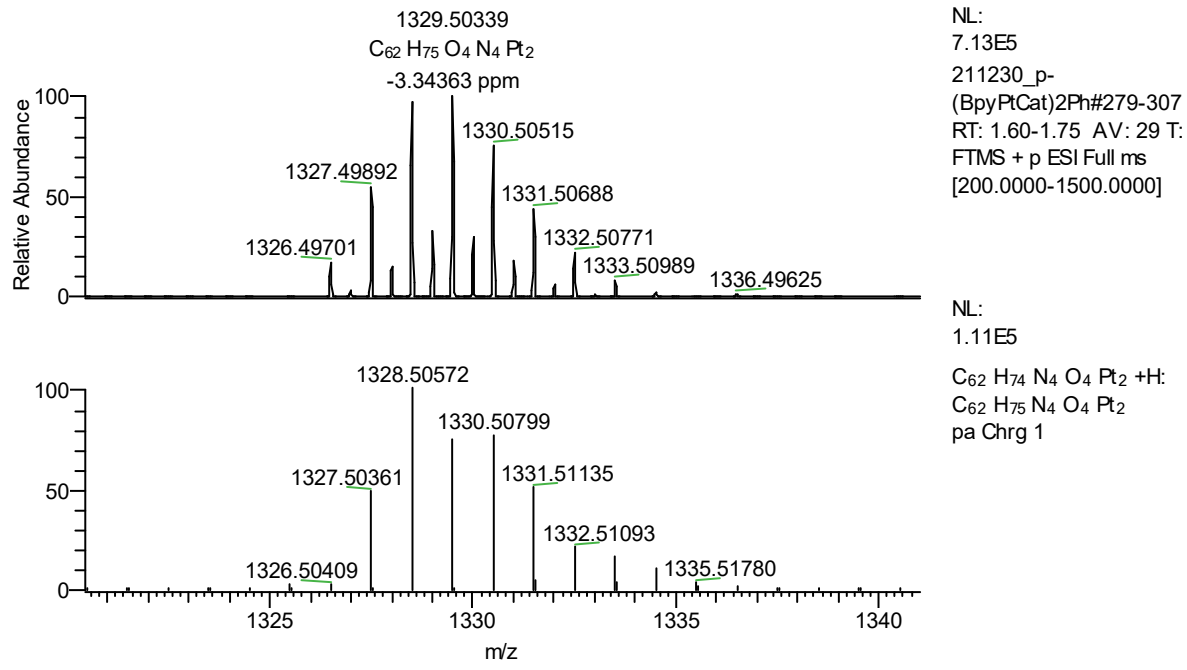

Figure S12. HRMS (ESI) data for ***p*-Ph[(CAT)Pt(bpy)]$_2$**. HRMS (ESI) m/z: $[M+H]^+$ Calcd for $C_{62}H_{74}N_4O_4Pt_2$ 1329.50559; Found 1329.50339. **A.)** Full scan Positive ion mode. **B.)** Experimental and theoretical isotopic distribution for $C_{62}H_{74}N_4O_4Pt_2$ $[M+H]^+$.

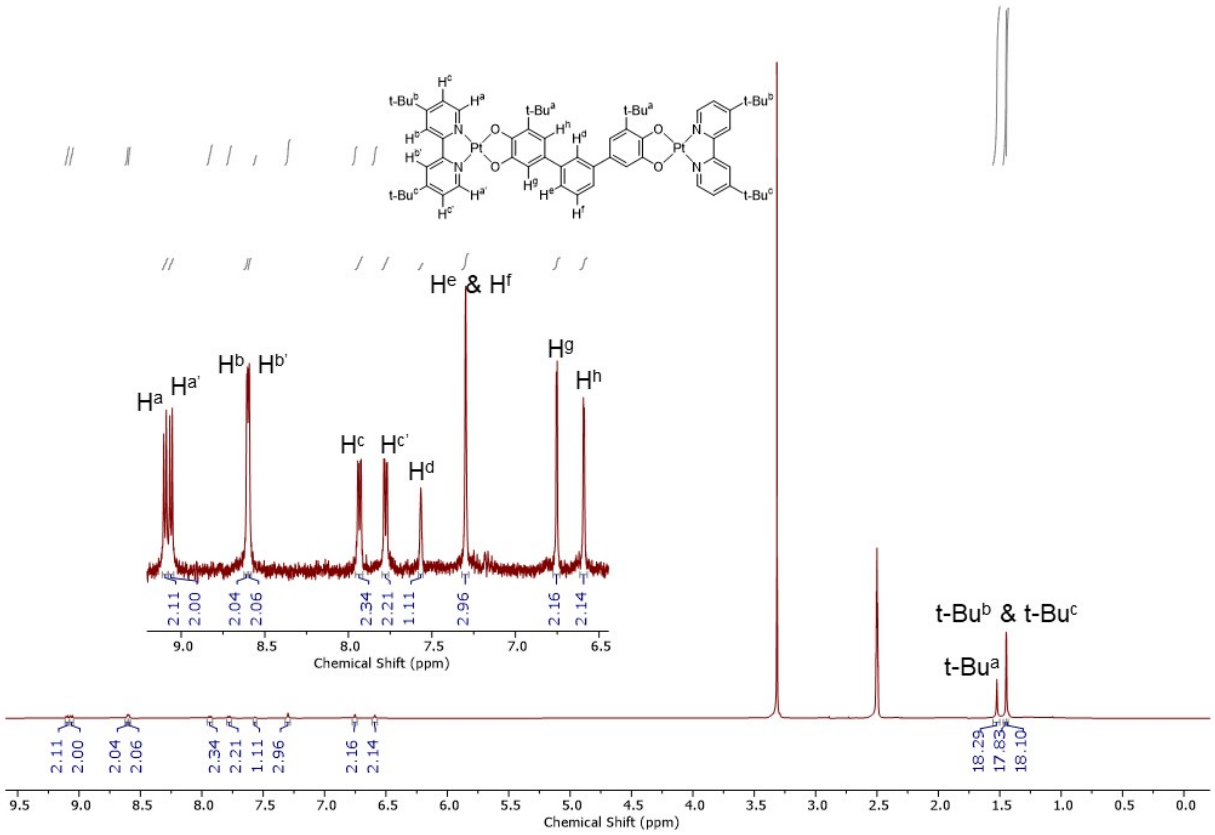

Figure S13. ^{1}H NMR spectrum of ***m*-Ph[(CAT)Pt(bpy)]$_2$**. ^{1}H NMR (400 MHz, DMSO) δ 9.10 (d, *J* = 6.13 Hz, 2H), 9.06 (d, *J* = 6.00 Hz, 2H), 8.61 (d, *J* = 1.75 Hz, 2H), 8.60 (d, *J* = 2.00 Hz, 2H), 7.93 (dd, *J* = 6.13, 2.00 Hz, 2H), 7.78 (dd, *J* = 6.13, 2.00 Hz, 2H), 7.57 (s, 1H), 7.30 (s, 3H), 6.75 (d, *J* = 2.13 Hz, 2H), 6.59 (d, *J* = 2.13 Hz, 2H), 1.52 (s, 18H), 1.45 (s, 18H), 1.45 (s, 18H). Impurities: water (3.31 ppm), unknown impurities (2.89, 2.73, 2.30, 1.17, 1.23, 1.07 ppm).

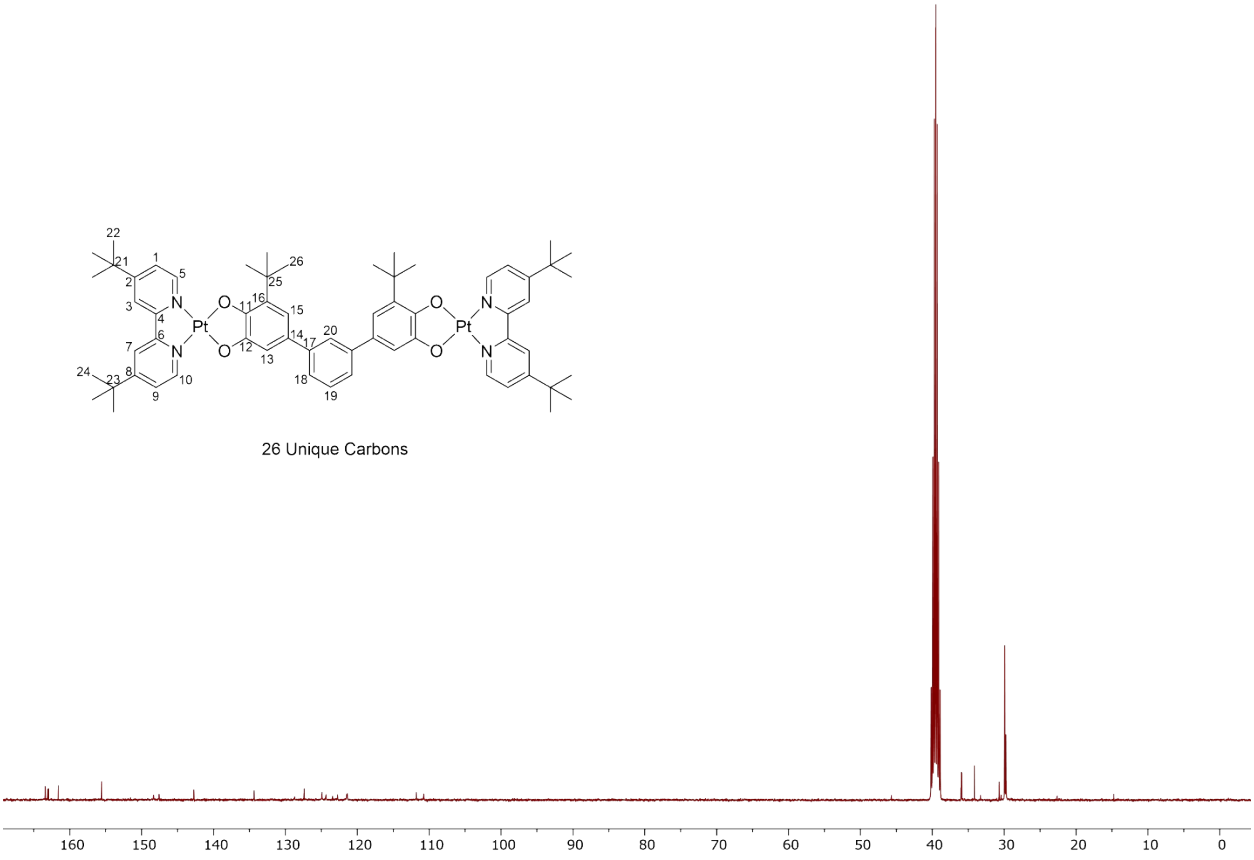

Figure S14. ^{13}C NMR spectrum of ***m*-Ph[(CAT)Pt(bpy)]$_2$**. ^{13}C NMR (101 MHz, DMSO) δ 163.41, 163.06, 162.93, 161.58, 155.56, 148.34, 147.58, 142.74, 134.36, 128.73, 127.39, 124.91, 124.35, 123.43, 122.74, 121.46, 121.37, 111.79, 110.76, 35.98, 35.92, 34.15, 30.70, 29.92, 29.76.

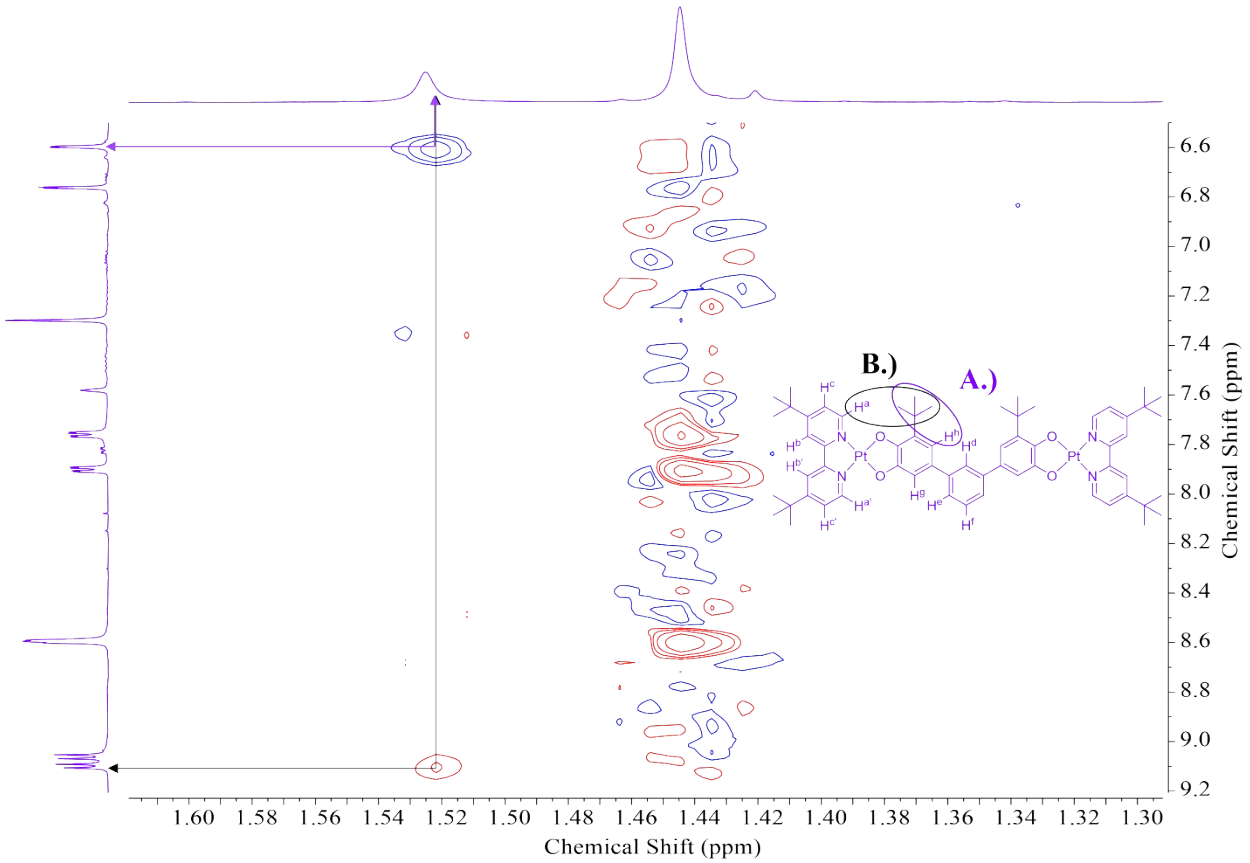

Figure S15. 2D NOESY spectrum of *m*-(BpyPtCat)$_2$Ph in DMSO-d$_6$ displaying A.) a NOE cross peak (1.52, 6.61 ppm) showing the dipole-dipole relaxation interaction between protons ortho to the catecholate tert-Butyl group and the catecholate *tert*-Butyl protons and B.) a NOE cross peak (1.52, 9.11 ppm) showing the dipole-dipole relaxation interaction between protons in the bipyridine 6 position and the catecholate tert-Butyl protons.

A.)

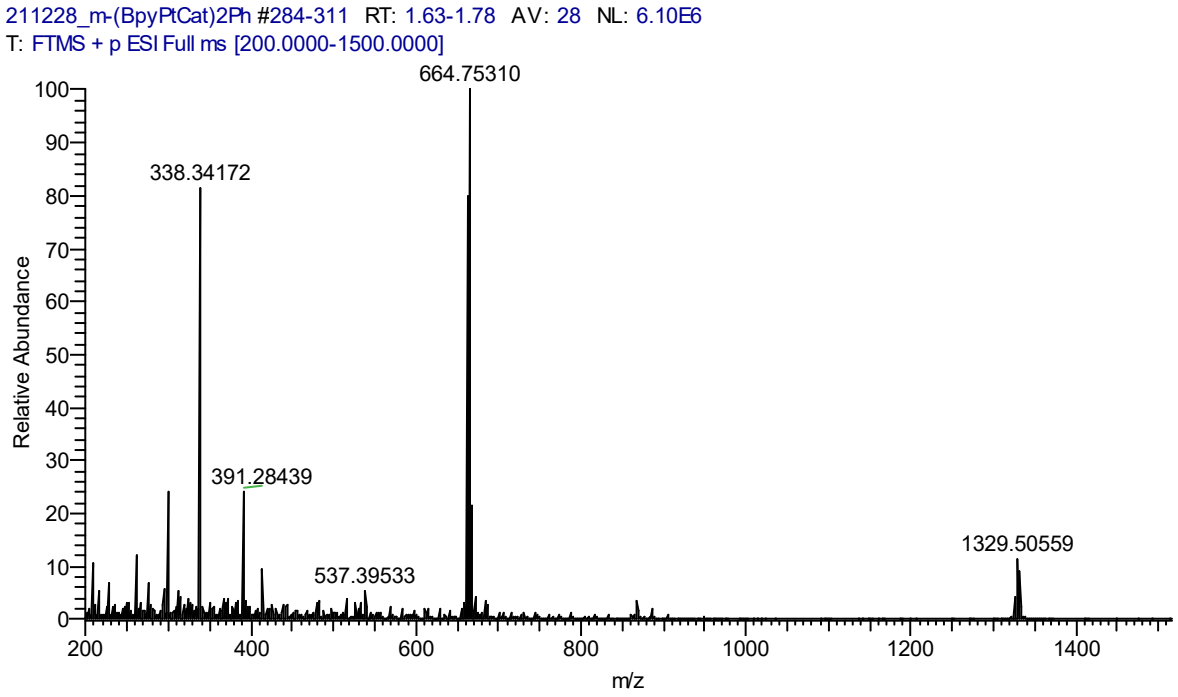

B.)

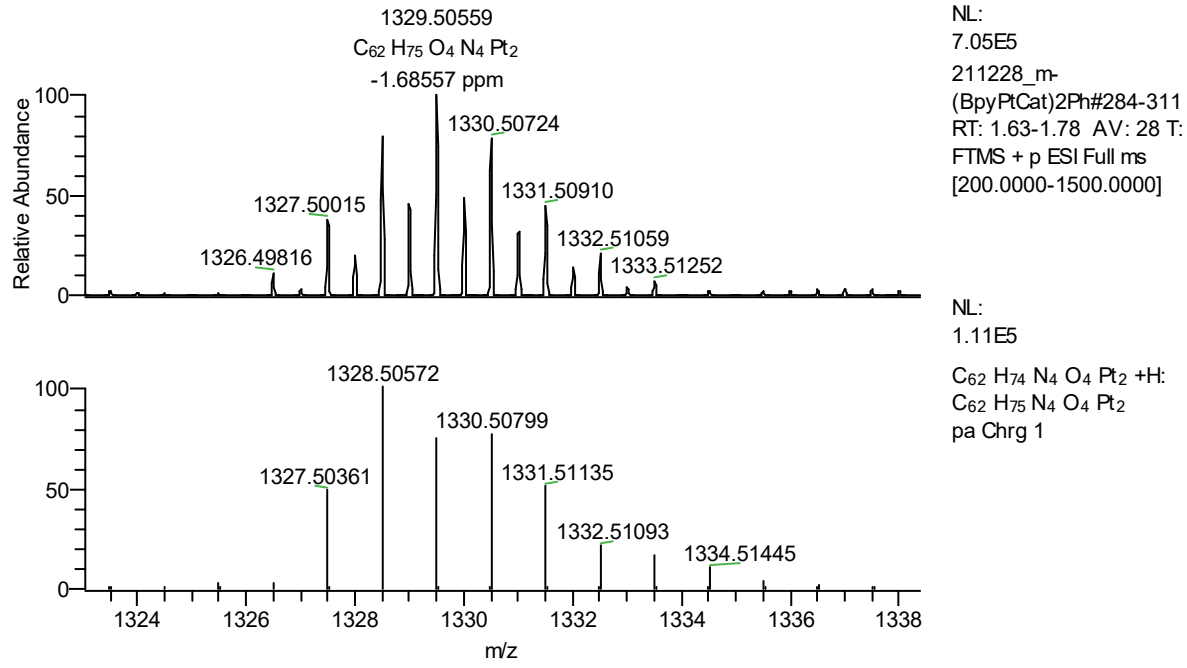

Figure S16. HRMS (ESI) data for *m*-(BpyPtCat)$_2$Ph. HRMS (ESI) m/z: $[M+H]^+$ Calcd for $C_{62}H_{74}N_4O_4Pt_2$ 1329.50559; Found 1329.50588. **A.)** Full scan Positive ion mode. **B.)** Experimental and theoretical isotopic distribution for $C_{62}H_{74}N_4O_4Pt_2$ $[M+H]^+$.